

A computer-based imaging system for multispectral inspection of skin cancer

Abstract. Multi-band imaging computer-based system, self-designed and self-constructed, based on a liquid-crystal filter with spectral transmittance driven in 400 nm - 740 nm wavelengths range is presented. Performed tests of images dimensionality reduction, which base on different types of principal component analysis, indicated onto flexibility and usefulness of the described approach for skin cancer diagnosis.

Streszczenie. W artykule opisano samodzielnie zaprojektowany i wykonany, wspomagany komputerowo, oparty na transmisyjnym filtrze ciekłokrystalicznym pracującym w zakresie długości fal od 400 nm do 740 nm, układ do obrazowania wielospektralnego. Przeprowadzone testy redukcji wymiarowości obrazu, w oparciu o różne rodzaje analizy jego składowych głównych, wskazały na użyteczność zastosowanego podejścia w diagnostyce raka skóry. (**Komputerowy system wielospektralnej analizy danych obrazowych raka skóry**).

Keywords: multispectral imaging, principal component analysis, spectral signature, skin cancer.

Słowa kluczowe: obrazowanie wielospektralne, analiza składowych głównych obrazu, sygnatura spektralna, rak skóry.

Introduction

Both in science and industry, different imaging procedures try to enhance or even correct human-eye red-green-blue (RGB) principal-components sensing-capabilities by the use of multi-photon microscopy [1], night-vision magnifiers [2] and/or imaging spectrometers [3]. One of the most important areas within this range of activity, is dedicated to multispectral imaging in a chosen spectral range, for example, in X-ray analysis [4], or in Fourier-Transform Infra-Red (FT-IR) spectroscopy. [5]

Within the visible range (VIS), multispectral imaging employs setups with mechanically selectable spectral windows [6], or electrically driven liquid-crystals (LCD) filters [7], and/or uses acousto-optic filtering [8,9]. VIS imaging applies different widths and combinations of spectral windows followed by computer-based image processing, which can be compatible with officially approved imaging standards. For example, in the VIS range, the Narrow Band Imaging (NBI) [10] standard is applied. NBI uses two or three bands, realized by sequentially switched light sources and vision detectors. The most frequently met 2-bands solution works within the two spectral regions, where: the central wavelength equals 415 nm and the full width at half maximum (FWHM) equals to 30 nm (a), and the central wavelength equals 540 nm and the FWHM is equal to 20 nm (b). The 3-bands NBI solution employs a set of three light sources at the following central-wavelengths and FWHM's: 415 nm (FWHM=30nm) (a), 445 nm (FWHM=30nm) (b), 500 nm (FWHM=30 nm) (c). In general, within NBI approach, the impact is imposed onto the electro-mechanical performance, both in relation to light-sources and image-capturing devices control.

Next, a more complicated approach can be realized by Multi-Band Imaging (MBI). Additionally, MBI can be compatible with the FICE (Fuji Intelligent Color Enhancement) standard [11]. This standard uses a digital image processing technique that enhances an appearance of analyzed structural-details by the use of RGB driven filters located very closely to CCD-sensor pixels. This standard employs 60 wavelengths, covering 400nm - 695 nm wavelength-range, incremented by 5 nm steps, which can be swept with an arbitrary, controllable sequence. In general, MBI approach concentrates on a captured-image analysis and relies on computer-based, intense, data computations. That solution is, however, relatively expensive.

Commonly, for all types of multispectral works, this step of image-data computations creates a separate, interesting

problem related to desired extraction of image information. Generally, an each solution for such analysis consists of: an input image segmentation [12,13], followed by denoising and image dimensional reduction [14,15], and finally, an image reconstruction [16,17]. Thus, these procedures lead to reduction of unwanted information, reduction of computer memory load, and a subsequent improvement of multispectral device performance.

In the current paper we present a newly designed and constructed opto-mechanical experimental setup, which goes beyond NBI standard, uses 21 spectral bands, captures naturally lit objects, and employs computer-based image processing. The implemented image-analysis procedures, leading to final human-eye-sensitive RGB image, can be automatic. This solution is relatively cheap and capable of working with diverse laboratory imaging devices.

Experimental setup

Multi-band imaging was implemented by the use of VariSpec liquid-crystal filter (CRI Inc.), for which the spectral transmittance was driven by the USB interface within the 400 nm - 740 nm wavelengths range. The transmitted wavelength was adjusted with 1nm accuracy. The filter was mounted in front of the variable focus Tamron 55-200mm F/4-5.6 lenses, followed by a thermoelectrically cooled, black&white, 1/8" (658 x 496 pixels) 'Luca' CCD camera manufactured by Andor Inc. Next, the self-made, afocal, two-lens system enabled the opto-mechanical coupling to the output optics of various devices (a microscope, camera lenses, endoscope etc.), and was mounted in front of the LCD filter (Fig.1).

The optimum filter performance was achieved for optical rays passing parallel to the device optical axis, therefore, for an image placed at infinity. The afocal system assured that by nature. The computer-controlled CCD camera enabled read-out of captured information from an every single pixel. The variable-focus lenses enabled adaptation of optical magnification to the optical characteristics of an arbitrary external device.

Examples of skin cancer images captured by the system are given in figure 2. It should be emphasized, however, that our directly captured images were black&white. Thus, the proper color scale of the device, depending on the LCD filter characteristics, the camera spectral sensitivity, and the spectral characteristic of applied light-sources, had to be found.

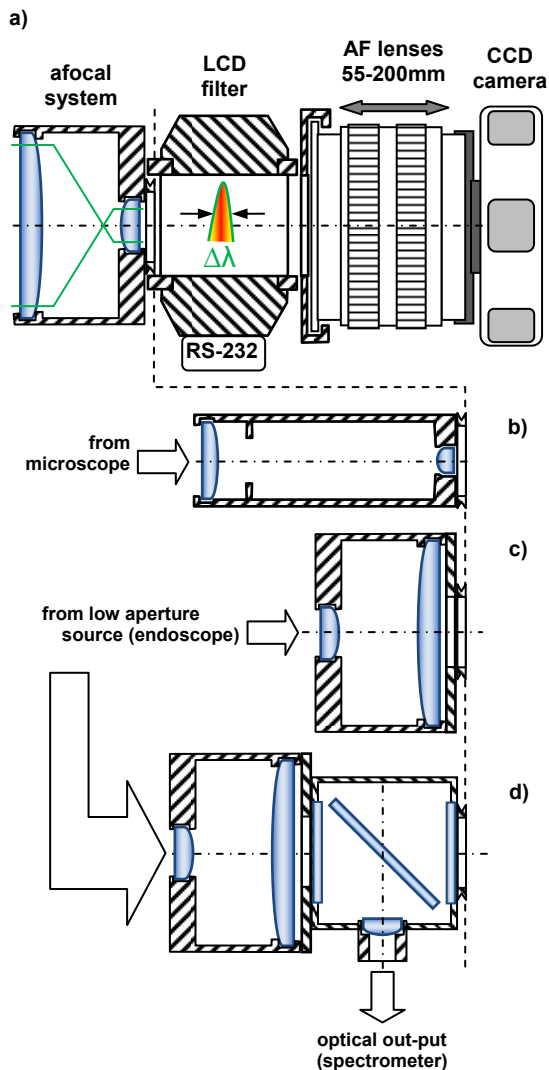


Fig. 1. Construction details of the opto-mechanical system (a), the afocal lenses can be substituted directly by a microscope ocular (b), by reversing the afocal lenses it can be coupled with a low-aperture device (c), or (for all above cases) the system can be modified by a beam-splitter to provide a fraction of signal to the optical spectrometer (d)

This is why we calibrated the device to the normalized spectral space on the basis of photographs captured from the referenced ColorChecker[®] set, manufactured by the GretagMacbeth company. This set of images created so-called training set. The ColorChecker[®] consists of patterned color sheets expressed by the normalized units defined by the International Commission on Illumination (CIE). We made separate images for each color, recorded captured pixels intensities (signatures) and transformed them into the normalized spectrum. The assumption of linear relations between the device spectral space and that normalized was applied. Thus, we took the classical least-mean square-method to determine the linear coefficients for that transformation [18]. Two approaches, called '*IvsI*' (one vs. one) and '*ALLvsI*' (all vs. one), were considered. For the '*IvsI*' spectrum, the value of the normalized space depends only on the corresponding single value of the device image-space. In contrast, in the '*ALLvsI*' approach, the normalized value consists of the linear combination of all device image-space values.

The results of calibration, expressed by the relative mean absolute error (*RMAE*). The comparison of the normalized spectra with the pattern is given in figure 3. In

the figure it is seen that the shorter wavelength range is noisy, what causes errors, especially for the '*ALLvsI*' method. The noise can be reduced, however, by the use of a more intense light source or by the elongation of CCD camera snapshot time.

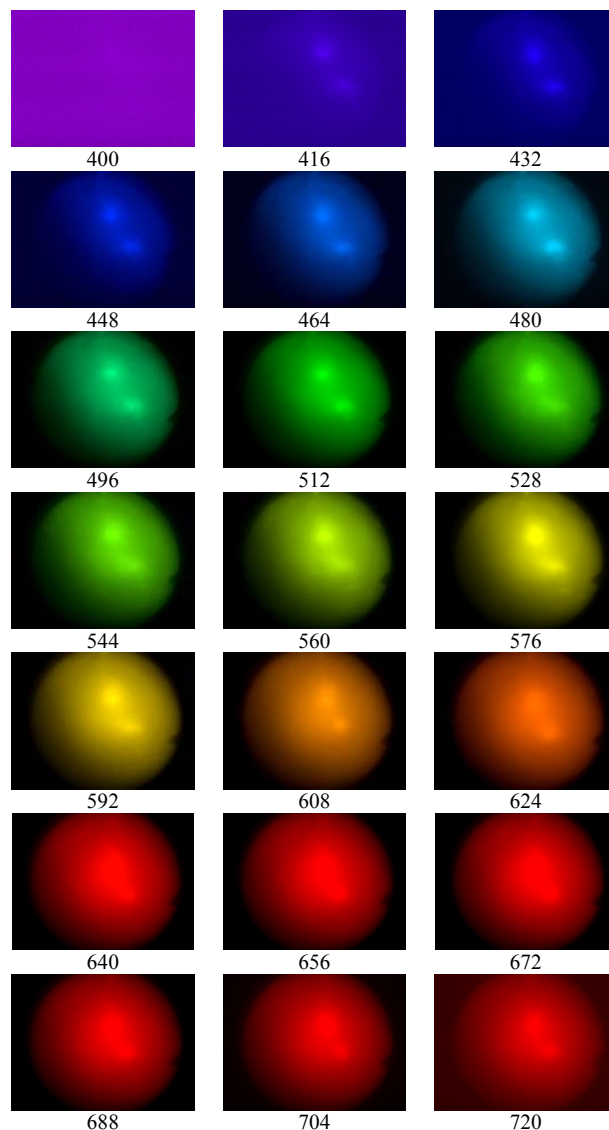


Fig. 2. A series of multispectral images obtained for skin tissue with centrally located cancer region. The numbers below figure are central wavelengths of transmitted bands expressed in nanometers

Numerical procedures and image analysis

In figure 2 captured images for the selected spectral bands (windows) are seen. The colored images are located strictly at spectral positions set by the LCD filter. It is evident that for some spectral bands information is not detectable. Thus, the proper multispectral information processing is needed for a reasonable reconstruction of images, keeping in mind the postulate of unwanted information reduction. Firstly, we should mention, that there is a real logistic problem with the elaboration of huge amounts of data stored in multi-dimensional color spaces. The problem results from the fact that an every pixel - one from 326368 (658 x 496) in our VGA-standard camera - collects spectral information from 21 spectral bands. This is why the reasonable reduction of that information to lower dimensional color-spaces, which preserves however, the majority of information, has to be carried out.

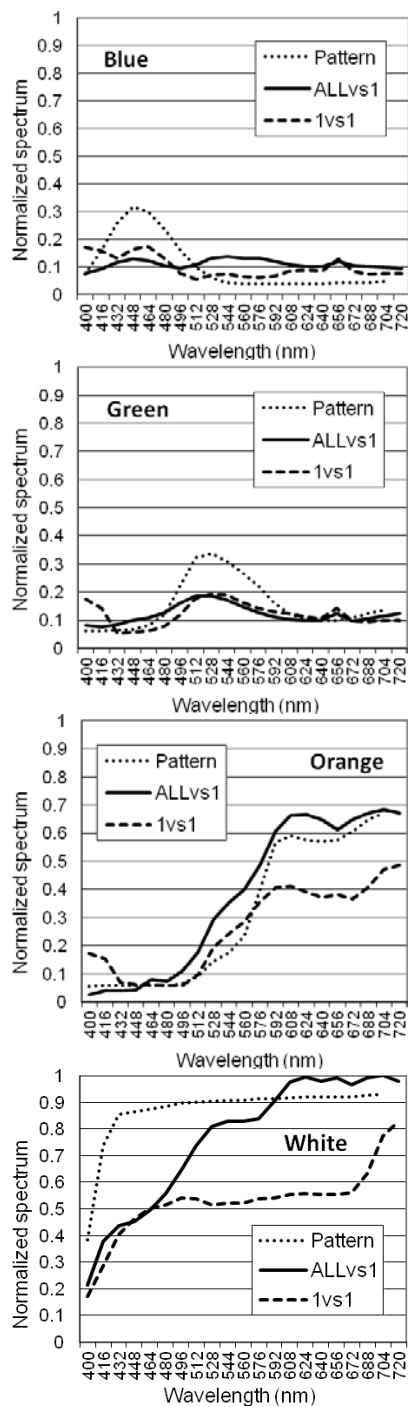


Fig. 3. Measured, during the training procedure, the normalized spectra of the selected colors; for blue, green, orange, and the white colors using the '1vs1' and the 'ALLvs1' methods. The registered spectra are compared with a standardized, ideal pattern. The 21 values of wavelengths, at abscissa, define the central positions of spectral windows used in experiments

In general, the solution of the problem is based on the assumption that some image attributes (intensities) are very often correlated each other, while some of them are quite random. There are plenty of dimensionality-reduction techniques. In general, they can be subdivided into the two main categories: the linear and nonlinear methods [19-21].

One of the most well known examples of linear method is the Principal Component Analysis (PCA), which applies the linear combinations of input image attributes, and tries to find the maximized variance of this combination.

The extension of the PCA method is the Kernel Principal Component Analysis (KPCA) - the nonlinear method [21].

The KPCA transforms quite easily the original image space using so-called kernel functions. Within our research efforts we tested both PCA and KPCA.

The above-mentioned dimensionality reduction techniques are based on the so called machine learning approach.¹⁸ Machine learning consists of two steps: (a) the above-mentioned training phase, (b) the working one, which reduces the input spectra and transforms it into the reduced image-space.

There is also another important issue related to the Kernel PCA approach. It has $O(n^2)$ computation complexity and the memory required to store the M matrix elements. It means in practice, that for the multispectral VGA image, and values coded with the double precision, over 700 gigabytes of memory are required. This is why, the number of elements in the training set has to be reduced. We can do this randomly or, for instance, we can select one row of every ten and one column of every ten. However, such an approach does not guarantee proper representation of the training set, since it could miss intrinsic image details. That is the reason to use the unsupervised classification²³ to explore spectral space clusters and to include, in the training set, only their geometric centers, instead of the selected spectral signatures. The number of 10^3 clusters seems to be sufficient to cover all the possible image objects and this requires only 7 megabytes of memory; 10^4 clusters requires 760 of megabytes, which is still acceptable. In our system we deployed a k -means algorithm for clustering,¹⁸ but the proposed approach allows application of any unsupervised classification technique.

To evaluate the effectiveness of dimensionality reduction performed the by PCA method we calculated aggregated, total variance cover of the given number of the first principal components. The results, given in figure 4, are satisfactory. Our visualization stores almost 55% of the input variance with a 14% compression ratio. Nevertheless, 45% of the variance is missed. To obtain variance cover above the 90% level, 13 attributes of the reduced space are required, while for the 95% level, 16 attributes are necessary.

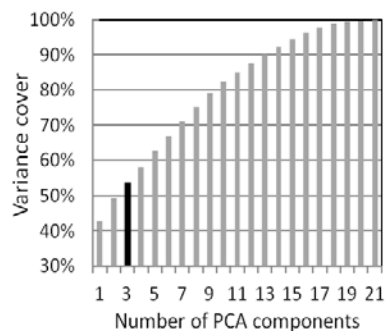


Fig. 4. The covariance cover as the function of the number of PCA attributes applied to the same image processing as that seen in figure 2. The case of three spectral attributes is marked (compare with figure 3)

In figure 5 we present results of an image dimensionality reduction for PCA and KPCA methods as well as for different types of normalization. For an every image cancer regions are clearly visible.

In the current work we presented a general purpose multispectral imaging device, designed and constructed from hand-made as well as commercially available parts. Our tests, based on PCA and KPCA reduction methods, show the usefulness of both approaches. For the presented region of interest the best quality image was obtained for the KPCA approach and the N2 normalization [22], since

internal structure details of cancer were localized. Importantly, such type of information is not detectable in normal procedures, thus for spectral channels treated independently.

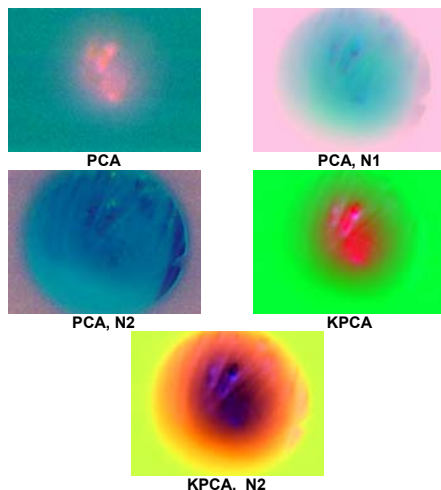


Fig. 5. Results of spectral signature dimensionality reduction for images presented in figure 1. Descriptions: KPCA – the reduction with the use of polynomial kernel function, N1, and N2 are symbols of normalization,²² respectively.

Acknowledgements

This work has been supported by The Polish National Science Center, projects 4272/B/T02/2009/36 and 4757/B/T02/2011/40.

REFERENCES

- [1] Pavlova I., Hume K. R., Yazinski S. A., Flanders J., Southard T. L., Weiss R. S., Webb W. W., Multiphoton microscopy and microspectroscopy for diagnostics of inflammatory and neoplastic lung, *J. Biomed. Opt.*, 17 (2012), 036014
- [2] Sabatini R., Richardson M. A., Cantiello M., Toscano M., Fiorini P., Jia H., Zammit-Mangion D., Night vision imaging systems design, integration, and verification in military fighter aircraft, *Proc. SPIE*, 8439 (2012), 84390R
- [3] Chen Y., Ji Y., Zhou J., Chen X., Wei X., Shen W., Wavelength calibration and spectral line bending determination of an imaging spectrometer, *Proc. SPIE*, 7384 (2009), 73841G
- [4] Haas W., Polyanskaya M., Bayer F., Gödel K., Hofmann H., Rieger J., Ritter A., Weber T., Wucherer L., Durst J., Michel T., Anton G., Hornegger J., Image fusion in x-ray differential phase-contrast imaging, *Proc. SPIE*, 8314 (2012), 83143U
- [5] Gawron W., Bielecki Z., Wojtas J., Stanaszek D., Lach J., Fimiarez M., Infrared detection module for optoelectronic sensors, *Proc. SPIE*, 8353 (2012), 83532U
- [6] Brauers J., Schulte N., Aach T., Multispectral Filter-Wheel Cameras: Geometric Distortion Model and Compensation Algorithms, *IEEE Trans. Imag. Process.*, 17 (2008), nr.1, 2368-2380
- [7] Kelly S. M., O'Neill M., in Handbook of Advanced Electronic and Photonic Materials and Devices, edited by Nalwa H. S., Volume 7: *Liquid Crystals, Display and Laser Materials* (Academic Press, 2000)
- [8] Yang Y., Sha X., Zhang Z., Analysis of the deviation of the diffracted beams caused by acousto-optic tunable filter in multispectral imaging, *Chin. Opt. Lett.*, 9 (2011), nr.8, 081101-081101
- [9] Hege E. K., O'Connell D., Johnson W., Bastys S., Dereniak E. L., Hyperspectral imaging for astronomy and space surveillance, *Proc. SPIE*, 5159 (2004), 380

- [10] Tanaka S., Sano Y., Aim to unify the narrow band imaging (NBI) magnifying classification for colorectal tumors: current status in Japan from a summary of the consensus symposium in the 79th Annual Meeting of the Japan Gastroenterological Endoscopy Society, *Digestive Endoscopy*, 23(Suppl. 1) (2011), 131-139
- [11] ASGE Technology Committee, Narrow band imaging and multiband imaging, *Gastrointestinal Endoscopy*, 67 (2008), nr.4, 581-589
- [12] Alev R. M., Fofanov V. B., Using segmentation to automate the interpretation of multispectral images, *J. Opt. Technol.*, 76 (2009), nr.12, 802-807
- [13] Guan T., Li L.-L., Zhang Y.-J., Competitive learning based on kernel functions and quadtree for image segmentation, *Proc. SPIE*, 8285 (2011), 82850Y
- [14] Van De Ville D., Nachtegaal M., Van der Weken D., Kerre E. E., Philips W., Lemahieu I., Noise Reduction by Fuzzy Image Filtering, *IEEE Trans. Fuz. Sys.*, 11 (2003), nr.4, 429-436
- [15] Shao X., Gao K., Lv L., Ni G., Unsupervised regions of interest extraction for color image compression, *Chin. Opt. Lett.*, 10 (2012), nr.01, 011001
- [16] Lu Y., Inamura M., Filtered Multiple Observation Image Superposition, Geoscience and Remote Sensing Symposium IGARSS '01, *IEEE 2001 International 3*, (2001), 1487-1489
- [17] Wenming G., Multi-layer Digital Images Superposition of High-power Micrograph, 2011 International Conference on Multimedia Technology (ICMT), (2011), 425-428
- [18] Witten I., Frank E., Data Mining: Practical Machine Learning. Tools and Techniques (Morgan Kaufmann Publishers, San Francisco, 2005)
- [19] Chuang Y.-K., Chen S., Delwiche S. R., Lo Y. M., Tsai Ch.-Y., Yang I-Ch., Hu Y.-P., Integration of independent component analysis with near infrared spectroscopy for evaluation of rice freshness, *Proc. SPIE*, 8369, (2012) 83690X
- [20] Yang J., Frangi A. F., Yang J., Zhang D., Jin Z., KPCA plus LDA: A complete kernel fisher discriminant framework for feature extraction and recognition, *IEEE Transactions on PAMI*, 27 (2005), nr.2, 230-244
- [21] Schölkopf B., Smola A., Learning with Kernels. Support Vector Machines, Regularization, Optimization, and Beyond (Massachusetts Institute of Technology, 2002)
- [22] Świtoński A., Błachowicz T., Zieliński M., Josiński H., Dimensionality reduction of multispectral images representing anatomical structures of an eye, in Proceeding of the International MultiConference of Engineers and Computer Scientists 2012, Editors: Ao S. I., Castillo O., Douglas C., Feng D. D., Lee J.-A., Vol. I (2012), 740-745, Newswood Limited, Hong-Kong, 2012.

Authors: Dr Eng. Adam Świtoński, Polish-Japanese Institute of Information Technology - Bytom Branch, Aleja Legionów 2, 41-902 Bytom, Silesian University of Technology, Faculty of Automatic Control, Electronics and Computer Science, Institute of Informatics, ul. Akademicka 16, 44-100 Gliwice, E-mail: adam.switonski@polsl.pl; Dr hab. Tomasz Błachowicz, prof. at SUT, Silesian University of Technology, Institute of Physics - CSE, ul. Krzywoustego 2, 44-100 Gliwice, E-mail: tomasz.blachowicz@polsl.pl; Prof. Dr hab. Eng. Aleksander Sieroń, Medical University of Silesia, Department and Clinic of Internal Diseases, Angiology and Physical Medicine, Center for Laser Diagnostics and Therapy, ul. Stefana Batorego 15, 41-902 Bytom, E-mail: sieron1@tlen.pl; Prof. Dr hab. Eng. Konrad Wojciechowski, Polish-Japanese Institute of Information Technology - Bytom Branch, Aleja Legionów 2, 41-902 Bytom, Silesian University of Technology, Faculty of Automatic Control, Electronics and Computer Science, Institute of Informatics, ul. Akademicka 16, 44-100 Gliwice, E-mail: konrad.wojciechowski@polsl.pl.